

We are grateful to B. I. Halperin, T. M. Rice, J. M. Rowell, and F. Stern for helpful conversations, and to J. V. Dalton, R. H. Doklan, and G. Kaminsky for the Si devices.

¹See, for example, J. L. Smith and P. J. Stiles, *Phys. Rev. Lett.* **29**, 102 (1972).

²F. F. Fang and A. B. Fowler, *Phys. Rev.* **169**, 619 (1968).

³N. F. Mott, *Electron. Power* **19**, 321 (1973).

⁴N. F. Mott and E. A. Davis, *Electronic Processes in Noncrystalline Materials* (Oxford Univ. Press, London, England, 1971).

⁵F. Stern, in "Critical Reviews in Solid State Sciences" (to be published), and unpublished; R. A. Abram, *J. Phys. C: Proc. Phys. Soc., London* **6**, L379 (1973), and references contained therein.

⁶F. Stern and W. E. Howard, *Phys. Rev.* **163**, 816 (1967).

⁷S. J. Allen, Jr., D. C. Tsui, and J. V. Dalton, *Phys. Rev. Lett.* **32**, 107 (1974).

⁸The source and drain are produced by diffusing phosphorus into the substrate to a level of $5 \times 10^{20}/\text{cm}^3$. The contact resistance is less than 10Ω in the temperature range of interest here. The resistance is determined by two-terminal measurements, so that one must carefully consider the possibility that the observed behavior may be due to contact effects between the source, drain, and channel. First, we cannot envision significant contact resistance in the properly fabricated MOSFET. Second, we have observed contact effects in some poorly fabricated MOSFETs and find that the contact problem manifests itself at large surface-electron

densities where the channel resistance drops substantially below the contact resistance. At low electron densities, high channel resistance, the contact resistance even in these rejected MOSFETs was no problem. Lastly, we note that there are documented in the literature four-terminal measurements at least down to 4.2°K that give the same threshold behavior as seen in two terminal measurements (see Ref. 2).

⁹A. B. Fowler, F. F. Fang, W. E. Howard, and P. J. Stiles, *Phys. Rev. Lett.* **20**, 901 (1966).

¹⁰F. F. Fang and A. B. Fowler, *Phys. Rev.* **41**, 1825 (1970).

¹¹Screening of the potential fluctuations by the free carriers should make E_c increase as n_s decreases. Potential fluctuations from surface roughness, however, might be expected to increase with n_s . The effect of electron-electron interactions on the dependence of E_c on n_s is not clear, but is probably important.

¹²The behavior of σ near E_c at $T=0$ has been a subject of controversy. While Mott proposes that σ is discontinuous at E_c with a minimum metallic conductivity, Cohen, Thouless, and Eggarter suggest that σ tends to zero continuously at E_c : See, for example, N. F. Mott, *Phil. Mag.* **26**, 1015 (1972); M. H. Cohen, *J. Non-cryst. Solids* **4**, 391 (1970), and *Phys. Today* **24**, 26 (1971); D. J. Thouless, *J. Non-cryst. Solids* **8/10**, 461 (1972); T. P. Eggarter, *Phys. Rev. A* **5**, 2496 (1972).

¹³J. T. Edwards and D. J. Thouless, *J. Phys. C: Proc. Phys. Soc., London* **5**, 807 (1972).

¹⁴E. P. Wigner, *Phys. Rev.* **46**, 1002 (1939), and *Trans. Faraday Soc.* **34**, 678 (1938); A. V. Chaplik, *Zh. Eksp. Teor. Fiz.* **62**, 746 (1972) [*Sov. Phys. JETP* **35**, 395 (1972)].

¹⁵M. Pepper, S. Pollitt, C. J. Adkins, and R. E. Oakley, *Phys. Lett.* **47A**, 71 (1974).

Theory of Angular Resolved Photoemission from Adsorbates

A. Liebsch

Department of Physics, University of Pennsylvania, Philadelphia, Pennsylvania 19174

(Received 1 April 1974)

A theory of the angular resolved photoemission from localized adsorbate orbitals is presented in which the effects of the final state are discussed in detail. Numerical results show a strong dependence of the energy-resolved angular distribution on the symmetry of the bonding orbitals and on the geometry of the adsorption site.

The recent experimental verification of the angular dependence in photoemission spectra¹ has stimulated considerable interest in this technique. In the case of clean surfaces, it is likely that information about the bulk energy bands and their possible modifications near the surface may be extracted from the angular and energy dependence. The purpose of this Letter is to demon-

strate that the angular distribution from localized adatom levels at the surface is dominated by the symmetry of the adsorption site as well as by the symmetry of the bonding orbitals.² This indicates the great potential of angular resolved photoemission as a tool complementary to low-energy electron diffraction (LEED) to analyze geometrical structures at surfaces.

The essential ingredient of our microscopic "one-step" model for the photoemission process lies in the description of the final state. Since the coherent elastic scattering of the excited electron by the periodic potential of the substrate is strong in the energy range of interest in photoemission, it is necessary to account for the full Bloch nature of the final state. Furthermore, the electronic mean free path at these energies is of the order of a few lattice spacings as a consequence of strong inelastic electron-electron interactions. It therefore appears natural to describe the final state by a multiple-scattering theory such as also has been applied in LEED calculations.³ The matrix elements between the localized initial and the complete final state are then evaluated numerically. The application of the same formalism for more complex initial states corresponding to emission from the substrate and to emission from hybridized substrate-adsorbate orbitals will be dealt with in a later publication. Also, no attempt has been made at this point to include the presence of the hole that is left behind by the excited electron.

The two processes that contribute to the scattering amplitude for the adsorbate signal are the

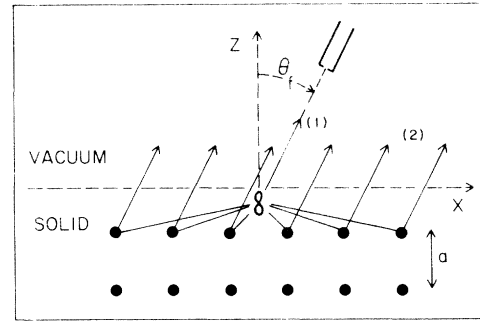


FIG. 1. Illustration of two processes contributing to photoemission from adsorbate p_z orbital: (1) direct emission into plane-wave final state, and (2) indirect emission via backscattering from substrate. Only single scattering from the first layer is indicated.

direct emission from the orbital into a plane-wave final state, $|\vec{k}_f\rangle$, and the indirect emission from the orbital via backscattering from the substrate lattice potential. Both are indicated schematically in Fig. 1. For a given polarization vector \vec{A} inside the solid and a photon energy $\hbar\omega$, the cross section is a function of final electron energy E_f and detector angles Θ_f and Φ_f . It is given by the expression

$$\sigma(E_f, \Theta_f, \Phi_f) \sim |\langle \vec{k}_f | (1 + TG) \vec{p} \cdot \vec{A} | \varphi_{\vec{R}} \rangle|^2 \delta(E_f - E_i - \hbar\omega). \quad (1)$$

Here, $\varphi_{\vec{R}}$ is the wave function of the orbital adsorbed at the site \vec{R} , E_i being its energy level; $T = V_L + V_L G T$ is the T matrix corresponding to the lattice potential V_L ; and G is a free-electron propagator with an appropriate self-energy inserted to include inelastic effects. The first term of the matrix element in Eq. (1), i.e., the direct emission in the absence of scattering, is simply proportional to the Fourier transform of the initial state:

$$\langle \vec{k}_f | \vec{p} \cdot \vec{A} | \varphi_{\vec{R}} \rangle = \exp(-i\vec{k}_f \cdot \vec{R}) \hbar \vec{k}_f \cdot \vec{A} F_{n_i}(|\vec{k}_f|) Y_{l_m}(\hat{k}_f), \quad (2)$$

where F_{n_i} and Y_{l_m} are the radial and the angular part of $\varphi(\vec{k}_f)$, respectively. The second term of the matrix element, i.e., the indirect emission from the adsorbate via backscattering from the substrate, can be evaluated for the general case of multiple elastic scattering and arbitrary atomic potentials.⁴ For simplicity, however, we present here only the result for single scattering from s -wave scatterers:

$$\begin{aligned} \langle \vec{k}_f | TG \vec{p} \cdot \vec{A} | \varphi_{\vec{R}} \rangle &\sim \exp(-i\vec{k}_f \cdot \vec{R}) F_{n_i}(|\vec{k}_f|) t(|\vec{k}_f|) \frac{1}{a^2} \sum_{\vec{g}} Y_{l_m}(k_{f\parallel} + \hat{g}, -k_{f\perp}(\vec{g})) \\ &\times \hbar [k_{f\parallel} + \hat{g}, -k_{f\perp}(\vec{g})] \cdot \vec{A} \frac{1}{-k_{f\perp}(\vec{g})} \frac{\exp(i\vec{g} \cdot d_{\parallel}) \exp[i\kappa(\vec{g})d_{\perp}]}{1 - \exp[i\kappa(\vec{g})a]}, \end{aligned} \quad (3)$$

where

$$\kappa(\vec{g}) \equiv -k_{f\perp}(0) - k_{f\perp}(\vec{g}), \quad (4a)$$

$$k_{f\perp}(\vec{g}) \equiv -[(2m/\hbar^2)(E_f + V_0 + i\Gamma) - (k_{f\parallel} + \hat{g})^2]^{1/2}. \quad (4b)$$

The \vec{g} 's are the reciprocal lattice vectors of the Bravais net parallel to the surface and a is the lattice constant. The normal and parallel position of the adatom relative to the substrate are denoted by d_{\perp} and d_{\parallel} , respectively. The quantity $t(|\vec{k}_f|)$ represents the s -wave component of a single-site scattering

vertex in the substrate, V_0 is the inner potential, and $\Gamma(E)$ is the imaginary part of the optical potential.

The above result exhibits the following physical features: (1) The contribution to the matrix element due to backscattering is no longer proportional to the angular part of the Fourier transform $Y_{lm}(\hat{k}_f)$ of the initial state. Instead, the expression involves the Fourier components corresponding to directions in k space that differ from \hat{k}_f by a reciprocal lattice vector parallel to the surface and that point into the crystal rather than to the detector. (2) Similarly, the matrix element is no longer proportional to $\vec{k}_f \cdot \vec{A}$ as in the absence of scattering but rather involves the factors $[k_{f\parallel} + \vec{g}_\parallel - k_{f\perp}(\vec{g})] \cdot \vec{A}$. (3) For a given detector angle, the structure in the intensity as function of final energy E_f is determined by the band structure of the substrate. In the specific case considered in Eq. (3), resonance energies occur for $\text{Re}\kappa(\vec{g})a = 2\pi n$, n integer, i.e.,

$$E_f + V_0 = E_{\parallel} + (E_n + E_{\vec{g}} + k_{f\parallel} \cdot \vec{g} \hbar^2/m^2)/4E_n, \quad (5)$$

where $E_n \equiv (\hbar^2 2\pi n/a)^2/2m$, $E_{\vec{g}} \equiv (\hbar \vec{g})^2/2m$, and $E_{\parallel} \equiv E \sin^2 \Theta_f$. These energies coincide with band crossings in the corresponding free-electron band structure. (4) The geometry of the adsorption site enters the matrix element only via two phase factors, one for the normal position d_{\perp} and one for the parallel displacement d_{\parallel} of the adatom relative to the underlying substrate. This is a particularly attractive feature since it permits the separation of adsorbate and substrate geometry: The positions at which extrema in the intensity occur are entirely determined by the symmetry of the substrate, whereas the relative intensities of these extrema are determined by the adsorption site.

In order to illustrate some of these features, we show in Fig. 2 the intensity as function of final energy for emission along the surface normal from an s orbital bound in two configurations.⁵ The curves represent the intensity for the case of single scattering (solid curves), multiple scattering (dotted curves), and in the absence of scattering (dashed curves). The three-dimensional reciprocal lattice vectors specify the resonance energies, Eq. (5), and the corresponding band crossings as indicated in the free-electron band structure at the top of the figure. The effect of backscattering from the substrate is seen to be of the order of 20–50% relative to the intensities in the absence of scattering. It is, however, rather remarkable that the multi-

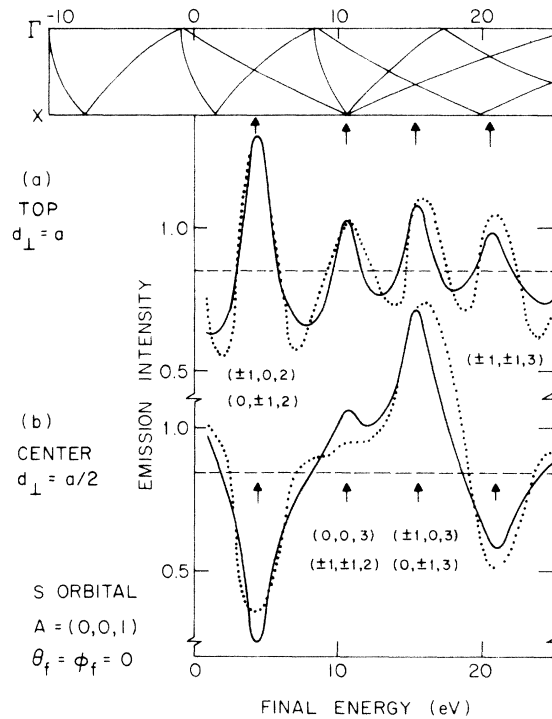


FIG. 2. Intensity (arbitrary units) as a function of final electron energy for emission from an s orbital adsorbed (a) in the position $(0,0,a)$ and (b) in the position $(a/2, a/2, a/2)$, relative to the substrate. Single scattering (solid curves), multiple scattering (dotted curves), and no scattering (dashed curves). The arrows indicate the resonance energies specified by the reciprocal lattice vectors, and the corresponding band crossings in the free-electron band structure at the top of the figure.

ple-scattering intensities agree so closely with the single-scattering intensities. We believe this to be a consequence of the fact that the single-scattering resonances coincide not only with the reflection points of the first band, as it is the case in LEED, but also with the intersections of the first band with all higher bands.⁶ This is because the adatom acts as a spherical source in contrast to the incoming plane wave in LEED. While this point requires further detailed study, it might prove to be of considerable practical interest in that single- or double-scattering approximations to the final state in photoemission from adsorbates are much more adequate than in LEED. Comparing panels (a) and (b), we notice that the change of the adsorption site from $(0,0,a)$ to $(a/2, a/2, a/2)$ inverts some of the maxima to minima because of the presence of the phase factors as described above.

It is apparent from Eq. (5) that in normal direc-

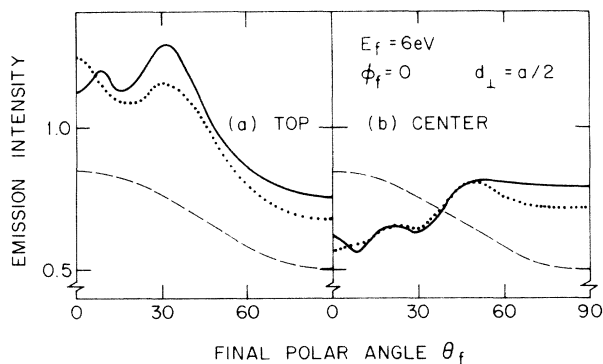


FIG. 3. Photoemission intensity (arbitrary units) as function of final polar angle for an s orbital adsorbed in (a) top and (b) center positions. Single scattering (solid curves), multiple scattering (dotted curves), and no scattering (dashed curves).

tion all resonances are degenerate with regard to various vectors \vec{g} whose components have opposite signs. At finite angles Θ_f and Φ_f , however, these resonances split very rapidly indicating that the photoemission intensity exhibits a strong angular dependence. As an example, Fig. 3 shows the intensity as function of polar angle Θ_f for two adsorption sites at a fixed energy E_f . In the absence of scattering, the intensity is a smooth function proportional to $\vec{k}_f \cdot \vec{A}$ (dashed curves). In the limit of single scattering (solid curves), the maxima that are seen in panel (a) for the top position are inverted into minima in panel (b) for the center position because of the phase factor associated with the parallel displacement. In both cases, the effect of multiple scattering (dotted curves) tends to smooth out the single-scattering intensities. Figure 4 shows, for the same geometries and the same energy, the intensity as function of azimuthal angle Φ_f at a polar angle of 32° . The fourfold symmetry of the substrate lattice clearly manifests itself in the intensity (solid curves) whereas in the absence of scattering the distribution is cylindrically symmetric (dashed curves). Again, multiple scattering [dotted curves, shown only in panel (a)] tends to smooth out the single-scattering intensities.

The results described above give strong support to the hope that the photoemission technique can be used to identify not only the bond orbitals of chemisorbed atoms but also the symmetry of adsorption site. One's hope in this matter is encouraged by the fact that single- or double-scattering approximations to the final state using

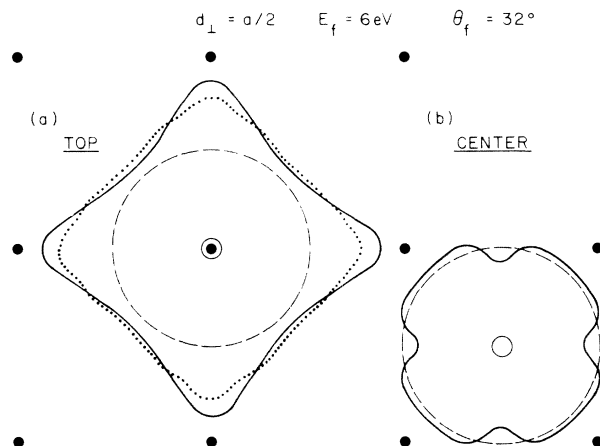


FIG. 4. Photoemission intensity (arbitrary units) as function of azimuthal angle for an s orbital adsorbed in (a) top and (b) center positions. Single scattering (solid curves), multiple scattering [dotted curve, shown only in panel (a)], and no scattering (dashed curves).

realistic atomic potentials appear to be adequate for a quantitative analysis of experimental data.

The author is grateful to Professor E. W. Plummer, Professor J. R. Schrieffer, and Dr. T. Gustafsson for many helpful discussions.

¹For a list of references on angular photoemission studies, see N. V. Smith and M. M. Traum, *Phys. Rev. Lett.* **31**, 1247 (1973).

²For photoemission from surface molecules into plane-wave final states, J. W. Gadzuk [*J. Vac. Sci. Technol.* **11**, 275 (1974), and to be published] has demonstrated that the angular resolved intensity is highly anisotropic reflecting both the adsorption geometry and the orientation of the chemisorption orbitals. While we believe the adequate description of the initial state to be crucial for a quantitative analysis of photoemission spectra, we restrict our discussion in the present Letter to localized adatom levels in order to isolate the angular anisotropy due to the Bloch character of the final state.

³For a review of LEED theories see, for example, G. E. Laramore, *J. Vac. Sci. Technol.* **9**, 625 (1972).

⁴A. Liebsch, to be published.

⁵All calculations are for the (001) surface of a simple cubic crystal and the following parameters are used: $V_0 = 10$ eV (inner potential), $\lambda_e = 12$ Å (electronic damping length), $\delta_s = \pi/2$ (s -wave phase shift), $a = 4$ Å (lattice constant), and $\vec{A} = (0, 0, 1)$. All curves are divided by $|\vec{k}_f| F_{nl}(|\vec{k}_f|)$ so that the intensity in the absence of scattering is energy independent. The initial energy can then be taken as arbitrary.

⁶The remaining crossings between higher-lying bands correspond to multiple-scattering resonances.